

# Study of Local Molecular Ordering in Layered Surfactant–Silicate Mesophase Composites

Li-Qiong Wang\* and Gregory J. Exarhos

Material Science Department, Pacific Northwest National Laboratory, Battelle Boulevard,  
Richland, Washington 99352

Received: June 28, 2002; In Final Form: October 15, 2002

We have synthesized layered surfactant–silicate mesophase composites using surfactant-templated synthetic routes under hydrothermal conditions. Local molecular ordering in both the bound surfactant and the inorganic framework for these mesophase composites has been observed and investigated using solid-state NMR and X-ray diffraction techniques. Synthesis parameters were systematically varied to determine the key factors that influence the molecular-ordering process. The dynamics and mobility of surfactant molecules at the interface have also been examined using NMR chemical-shift analyses, relaxation-time studies, and 2D WISE measurements. Results from this current work are compared with studies reported on other surfactant–silicate mesoporous materials.

## 1. Introduction

The discovery of the M41S series of mesoporous materials<sup>1,2</sup> has generated great interest in the scientific community because of their unique properties and many potential applications in catalysis, adsorption, and separation. These materials have high surface areas ( $> 1000 \text{ m}^2/\text{g}$ ), ordered pore structures, extremely narrow pore-size distributions, and variable pore diameters from 2 to 30 nm. Various mechanisms for the syntheses and formation of these materials have been reported.<sup>1–13</sup> The formation of such mesoporous materials is generally attributed to a “templating” effect of surfactant molecules although silicate species in solution also play an important role in the ordering of surfactant molecules at interfaces.<sup>5–7</sup> Preparation methods involve mixing silica precursors (such as sodium aluminate, tetramethylammonium silicate, TEOS, or silica) in a surfactant-containing (cetyltrimethylammonium chloride, CTAC, or cetyltrimethylammonium bromide, CTAB) solution and treating the mixture at temperatures below  $150^\circ\text{C}$ . Surfactants usually self-organize into micellar phases, the most common of which consists of rodlike micelles packed in hexagonal arrays. The ceramic precursors subsequently bind to the headgroups of the surfactant molecules, forming a continuous surfactant–silicate mesophase. The surfactant molecules can then be removed by thermal or chemical treatment. The size and chemical nature of surfactant headgroups can be varied to obtain controlled architectures typified by mesoscopically ordered lamellar (MCM-50), hexagonal (MCM-41), or cubic (MCM-48) phases.<sup>13</sup> Although these materials show long-range periodic ordering, they lack short-range or local molecular ordering in their inorganic silica frameworks. Unlike crystalline zeolites, where high-level ordering is present, both X-ray diffraction and  $^{29}\text{Si}$  NMR data reveal disordered amorphous frameworks in these surfactant–silicate mesophase composites.<sup>1–13</sup>

To promote both selectivity for molecular adsorption and separation processes and catalytical activity, a locally ordered zeolite-like framework in the mesoporous material is highly desirable. Thus far, few studies have reported successful syntheses of homogeneous mesophase composites with both

local molecular and mesoscopic ordering.<sup>14–17</sup> The ability to make such materials has been difficult because synthetic approaches for combining a long-range-ordered mesophase with a locally ordered zeolite-type material are rather demanding. In general, syntheses of crystalline zeolite materials require shorter surfactant molecules and higher temperatures ( $> 150^\circ\text{C}$ ), whereas most mesophase composites are synthesized with longer surfactant molecules at lower temperatures ( $< 150^\circ\text{C}$ ). High-temperature approaches for the synthesis of such materials likely will lead to surfactant decomposition resulting in the collapse of the long-range-ordered mesostructure. Many previous studies have used long surfactant molecules and small amines together under different hydrothermal treatments to make mesoporous materials with zeolite-like inorganic frameworks.<sup>14–16</sup> Unfortunately, the final products are often inhomogeneous materials composed of a segregated mixture of MCM-41 and zeolite crystalline materials. Only very recently has one study shown success in making the layered surfactant–silicate mesophase composites with local molecular ordering in the resident inorganic framework.<sup>17</sup> However, these materials are not the crystalline zeolite-like materials that are highly desired by industry because they lose local molecular ordering upon calcination.

There has been a considerable research effort over the last 10 years to address the formation mechanism for mesoporous materials. However, little effort has been devoted to the understanding of the local-molecular-ordering phenomenon in both the bound surfactant and the evolving inorganic framework. Several key factors influence molecular structure formation in the final products. These include (1) the nature of the surfactant molecule, which is defined by the resident chemical groups, the chain length of the surfactant molecule, and the size of the headgroup; (2) the degree of polymerization of the silicate framework, which depends on the pH and the type of silica precursors used in the synthesis; (3) interfacial interactions between the surfactant and silica precursor species, which are directly related to the molar ratio of surfactant to silica; and (4) physical conditions during reaction such as temperature or water content. The critical factors that influence local molecular ordering must be identified for reliable syntheses of these ordered systems.

\* Corresponding author. E-mail: lq.wang@pnl.gov.

Local molecular ordering in surfactant–silicate mesophase composites can be probed by a variety of nuclear magnetic resonance (NMR) techniques since NMR is sensitive to the local chemical environment. Solid-state  $^{29}\text{Si}$  NMR spectroscopy has been used to characterize the extent of crystallization and evolution of the silica framework,<sup>1,5,13,17–19</sup> whereas solid-state  $^{13}\text{C}$  spectroscopy is used to determine the local structure, conformational ordering, and dynamics of surfactant molecule organization in as-synthesized surfactant–silicate mesophase composites with amorphous frameworks.<sup>1,18,20</sup> Thus far, no NMR studies have been reported on as-synthesized mesophase composites with local molecular ordering in their frameworks. Since the surfactant ordering at the silicate solution interface and the nature of the interaction between surfactant and the silica surface are the key issues in understanding the formation mechanisms, information regarding the structural and dynamic properties of surfactant molecules at the molecular level is required to provide further insight into these issues. Therefore, it is important to examine local molecular ordering not only in the inorganic framework but also in that associated with surfactant organization.

This work reports a molecular-level investigation of local-ordering phenomena in both the surfactant organization at interfaces and in the inorganic framework for surfactant–silicate mesophase composites. The layered surfactant–silicate mesophase composites with local molecular ordering have been synthesized using surfactant-templated synthetic routes under hydrothermal conditions. Although these materials that are similar to the materials synthesized in the previous study<sup>17</sup> are not the true crystalline zeolite-like materials, they offer an opportunity to investigate local molecular ordering associated with their surfactant organization and inorganic framework in as-synthesized mesoporous materials. Such information will be useful in future studies focused on the synthesis of true crystalline mesophase materials. In the work reported here, synthesis conditions were varied to determine the key factors that influence local molecular ordering. The dynamics and mobility of surfactant molecules at interfaces have also been examined using NMR chemical-shift analyses, the relaxation time  $T_{\text{CH}}$  (cross-polarization time constant), and 2D wide-line separation (2D WISE) measurements. Results from the current study are compared with those derived from other surfactant–silicate mesoporous materials.

## 2. Experimental Section

**Synthesis.** Raw materials used in the synthesis were alkyl-trimethylammonium surfactants:  $\text{C}_{16}\text{H}_{33}(\text{CH}_3)_3\text{NBr}$  (CTAB) or  $\text{C}_{10}\text{H}_{21}(\text{CH}_3)_3\text{NBr}$  from Fisher, tetraalkylammonium hydroxides including tetramethylammonium hydroxide (TMAOH, 25 wt % in  $\text{H}_2\text{O}$ , Alfa), tetrapropylammonium hydroxide (TPAOH, 20 wt % in  $\text{H}_2\text{O}$ , J. T. Baker Chemical Co.), and tetrabutylammonium hydroxide (TBAOH, 40 wt % in  $\text{H}_2\text{O}$ , Alfa), Hi-Sil 233 (aggregates of 20-nm amorphous silica particles, PPG Industries) silica, and deionized water. Processing parameters were varied to evaluate their influence on directing local ordering. First, samples with three different molar ratios (0.2:1, 1:1, and 4:1) of TMAOH/CTAB were prepared while keeping the molar ratio of  $\text{SiO}_2$ /CTAB fixed at  $\sim 3$ . A typical molar chemical composition for a 1:1 TMAOH/CTAB sample is 1.0 CATB/3.0  $\text{SiO}_2$ /1.0 TMAOH. Synthetic procedures for preparing these samples involve dissolving solid CTAB in water to make a 25 wt % surfactant solution by stirring the mixture for 30 min and heating in a 60 °C water bath for 10 min if necessary. Then a TMAOH (25 wt %) solution and  $\text{SiO}_2$  (from

Hi-Sil 233) particles were added to the surfactant solution and stirred for an additional 60–120 min. The resulting mixture was placed in a small, sealed, Teflon-lined hydrothermal reactor and processed at 150 °C for 24 h. The reaction products were allowed to cool to room temperature and then thoroughly washed with DI water to elute excess surfactant and TMAOH solution. The final dried materials through vacuum filtration were used for solid-state NMR measurements. Other samples were synthesized using TPAOH and TBAOH instead of TMAOH under otherwise similar conditions. In addition, samples were also made using  $\text{C}_{10}\text{H}_{21}(\text{CH}_3)_3\text{NBr}$  as a surfactant instead of CTAB.

**Characterization.** Solid-state 75.0-MHz  $^{13}\text{C}$  MAS (magic-angle spinning) NMR experiments were carried out with a Chemagnetics spectrometer (300 MHz, 89-mm-wide bore Oxford magnet) using a variable-temperature double-resonance probe. Both single-pulse (SP) Bloch-decay and cross-polarization (CP) methods were used with  $^1\text{H}$  decoupling. Cross-polarization time constant  $T_{\text{CH}}$  values were obtained using variable-contact-time  $^{13}\text{C}$  CP MAS NMR.<sup>20</sup> Samples were loaded into 7-mm Zirconia PENCIL rotors and spun at 3–4 kHz. Spectra were collected by using a single-pulse (SP) excitation Bloch decay method with a 4.5- $\mu\text{s}$  (90°)  $^{13}\text{C}$  pulse and a repetition delay of 10 to 60 s. For all experiments, a 40-ms acquisition time and a 50-kHz spectral window were employed. The number of transients was 1000–3000. The power levels of the carbon and proton channels were set so that the Hartmann–Hahn match was achieved at 55 kHz in our variable-contact-time experiments. A Lorentzian line broadening of 24 Hz was used for all  $^{13}\text{C}$  spectra. Solid-state 59.3-MHz  $^{29}\text{Si}$  MAS NMR spectra were also taken for all samples spun at 3–4 kHz the using single-pulse (SP) Bloch decay method with  $^1\text{H}$  decoupling. A Lorentzian line broadening of 50 Hz and a 30-s repetition delay were used for  $^{29}\text{Si}$  spectra. Tetramethylsilane (TMS) was used directly as a chemical-shift reference in both  $^{13}\text{C}$  and  $^{29}\text{Si}$  NMR spectra.

Two-dimensional wide-line separation NMR spectroscopy was also used in this study. In a 2D WISE pulse sequence,<sup>21</sup> a  $^1\text{H}$  90° pulse was applied and followed by an incremented proton evolution period  $t_1$ . After each  $t_1$  period, cross polarization (CP) was followed by a TOSS (total suppression of spinning sidebands) sequence.<sup>22</sup> The subsequent carbon detection with proton decoupling gives a modulated  $^{13}\text{C}$  spectrum as a function of  $t_1$  due to the free-induction decay of the associated protons. The 2D Fourier transform gives a 2D spectrum with high-resolution  $^{13}\text{C}$  CP MAS spectra in one dimension and the proton wide-line spectra associated with each carbon in the other dimension. In our measurements, a 90° pulse width for both the  $^1\text{H}$  and  $^{13}\text{C}$  pulses was 4.5  $\mu\text{s}$ . The  $^{13}\text{C}$  CP MAS spectra were taken with a contact time of 0.15 ms and a pulse delay of 3 s. The 2D data had a size of 128 points in the  $t_1$  ( $^1\text{H}$ ) dimension and 1K data points in the  $t_2$  ( $^{13}\text{C}$ ) dimension. The spectrum width in  $t_1$  was 200 kHz (dwell time of 5  $\mu\text{s}$ ) and 20 kHz in  $t_2$  (dwell time 50  $\mu\text{s}$ ). Amplitude spectra from the Fourier transform were used for the proton dimension ( $^1\text{H}$ ).

Samples for transmission electron microscopy (TEM) were prepared by ultramicrotomy. Microtomy was conducted on an NT 6000 ultramicrotome (Sorval) with a Microstar diamond knife. TEM characterization was performed on a Philips 400 or Joel 1200 microscope at 120 kV. X-ray diffraction (XRD) patterns of powder samples were measured with a Philips model XRG-3100 X-ray diffractometer with  $\text{Cu K}\alpha$  radiation using a  $2\theta$  range of 1–45° with a 0.05°/10 s scan rate. TEM and XRD results reported here were obtained from samples prior to calcination.

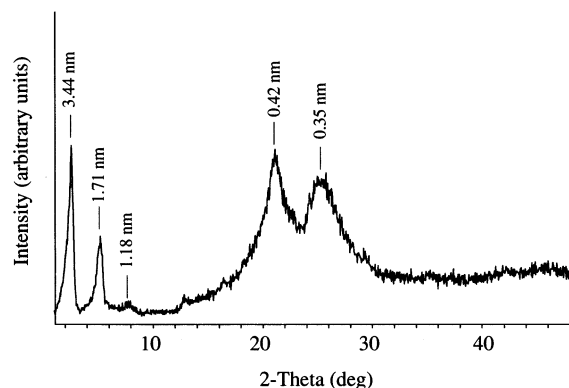


**Figure 1.** X-ray diffraction patterns for surfactant-silicate mesophase composites with a 1:1 molar ratio of TMAOH/CTAB.

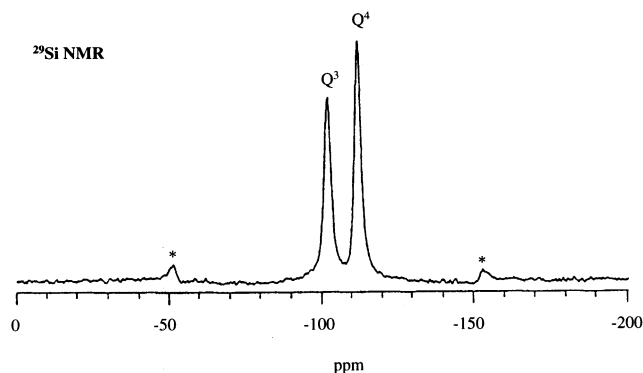


**Figure 2.** Single-pulse (SP) solid-state  $^{29}\text{Si}$  NMR spectra with  $^1\text{H}$  decoupling along with the peak assignments (\* denotes spinning sidebands) for CTAB-silicate mesophase composites with a 1:1 molar ratio of TMAOH/CTAB.

### 3. Results and Discussion

Local-molecular-ordering processes associated with surfactant organization and the inorganic framework are influenced by many factors. A previous study has reported the dependence of surfactant headgroup size and chemistry on local molecular ordering in the inorganic framework for layered surfactant-silicate mesophase composites.<sup>17</sup> In this section, however, we examine the influence of several critical factors including the temperature, the length of the surfactant chains, and the relative amount of TMAOH to surfactant on the local molecular ordering not only in the framework but also in the bound surfactant.

Figure 1 displays the X-ray diffraction pattern for the surfactant-silicate mesophase composite prepared with a 1:1 molar ratio of TMAOH/CTAB under hydrothermal conditions at 150 °C. Three distinct low-angle 100, 200, and 300 reflections observed at 3.44, 1.71, and 1.18 nm, respectively, indicate a mesoscopically (or long-range) ordered lamellar phase, in agreement with TEM micrographs (not shown here) taken for this material. Furthermore, local molecular ordering in the silica framework for this material is revealed in its  $^{29}\text{Si}$  NMR spectrum given in Figure 2, where two well-resolved narrow resonances at -102 ppm ( $\text{Q}^3$ ) and -112 ppm ( $\text{Q}^4$ ) (fwhm < 3 ppm) with a small shoulder at -90 ppm ( $\text{Q}^2$ ) are observed. In contrast, for typical M41S and other surfactant-silicate mesophase composites,<sup>1,5,13,17-19</sup>  $^{29}\text{Si}$  NMR spectra give three inhomogeneously broadened  $^{29}\text{Si}$  resonances centered at -90, -100, and -109 ppm (fwhm = 9 ppm), characteristic of an amorphous silica framework. The broad overlapping resonances observed for amorphous silica result from the inhomogeneous distributions of Si-O-Si bond angles and bond lengths in the locally disordered silica framework. Thus, two unusually narrow  $^{29}\text{Si}$

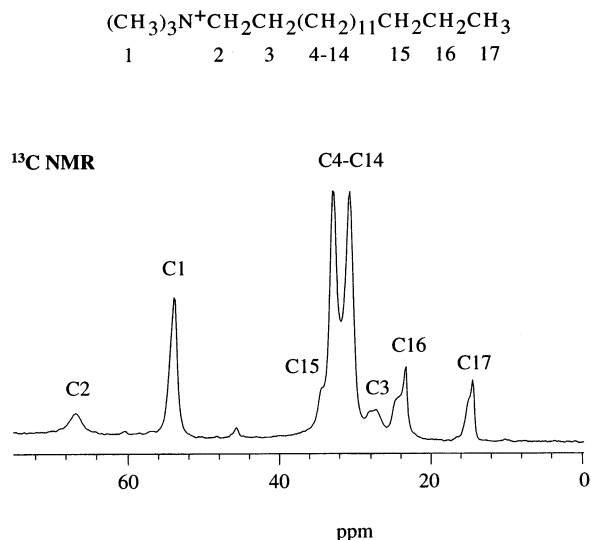


**Figure 3.** Single-pulse (SP) solid-state  $^{13}\text{C}$  NMR spectra with  $^1\text{H}$  decoupling along with the peak assignments for CTAB-silicate mesophase composites with a 1:1 molar ratio of TMAOH/CTAB. The peak splittings in resonances associated with C3, C16, and C17 groups are due to conformation heterogeneity.

resonances illustrated in Figure 2 suggest a high degree of local molecular ordering in the silica framework for the 1:1 TMAOH/CTAB surfactant-silicate mesophase composite. In general,  $^{29}\text{Si}$  resonances at approximately -90, -100, and -109 ppm are assigned to  $\text{Q}^2$ ,  $\text{Q}^3$ , and  $\text{Q}^4$   $^{29}\text{Si}$  species, respectively, where the superscript represents the number of silicon atoms covalently bonded to a silicon atom through bridging oxygen atoms.<sup>23</sup> The degree of polymerization for such silica frameworks is proportional to the relative number of  $\text{Q}^4$  species in the network. The very small number of  $\text{Q}^2$  species observed in Figure 2 indicates a higher degree of silica polymerization in the framework for the 1:1 TMAOH/CTAB surfactant-silicate mesophase composite than for the typical M41S type of mesoporous material.<sup>1,2</sup>

Since most of the MCM-41 materials<sup>13</sup> without local molecular ordering were made at 100 °C using a nearly identical chemical composition to that used in the synthesis for the 1:1 TMAOH/CTAB mesophase composite prepared in this study, the key difference appears to be the temperature used in the respective synthesis methods. A higher temperature was chosen in our synthesis in order to test whether local molecular ordering is enhanced at increased processing temperature. Indeed, our results show that the higher temperature chosen in our synthesis increases local molecular ordering in the silica framework. It is not surprising to see increased local molecular ordering in the silica framework because it is well known that higher temperatures are required to make crystalline zeolite materials. However, such temperature effects on the local ordering process in the surfactant organization have not been investigated previously. Since surfactant molecules are believed to act as a template in the synthesis of surfactant-silicate mesophases, it is important to examine such temperature effects on the organization and dynamics of surfactant molecules in the locally ordered silica framework.

The ordering and dynamics of surfactant molecules at interfaces in this study were probed using a variety of  $^{13}\text{C}$  solid-state NMR techniques. Figure 3 shows a single-pulse (SP) solid-state  $^{13}\text{C}$  NMR spectrum for the 1:1 TMAOH/CTAB surfactant-silicate mesophase along with the peak assignments based on the previous studies.<sup>18,20</sup> This  $^{13}\text{C}$  NMR spectrum confirms that surfactant molecules remain intact under a 150 °C hydrothermal treatment. Thus, our choice of 150 °C, which is higher than



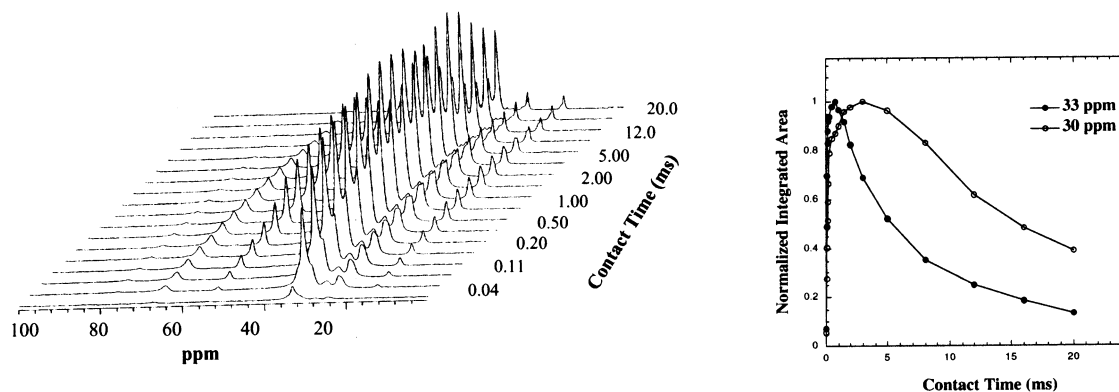


**Figure 4.** Contact-time array spectra and their corresponding plots of integrated peak areas for 31.0 and 33.2 ppm resonances as a function of the  $^1\text{H}$ – $^{13}\text{C}$  cross-polarization contact time.

most temperatures used in the syntheses of mesoporous materials without local molecular ordering, is appropriate because at this temperature the local ordering in the silica framework increases while both the surfactant molecules and mesostructures remain intact. In comparison with previous  $^{13}\text{C}$  NMR spectra for as-synthesized M41S-type materials,<sup>1,18,20</sup> Figure 3 displays a strikingly unique feature in the  $^{13}\text{C}$  NMR spectrum for the 1:1 TMAOH/CTAB surfactant–silicate mesophase composite. Instead of the expected single, dominated resonance at  $\sim 30$  ppm, which is associated with the internal methylenes (C4–C14) of surfactant molecules in amorphous silica,<sup>1,18,20</sup> two large, well-resolved narrow resonances appear at 31.0 and 33.2 ppm, both of which are assigned to the internal methylene groups (C4–C14) for the 1:1 TMAOH/CTAB surfactant–silicate mesophase.

Local ordering in the bound surfactant can now be determined from the degree of the ordered (all-trans) conformation versus the degree of the disordered (gauche) conformation of surfactant molecules in the surfactant–silicate mesophase. The relative population of trans versus gauche conformations of surfactant molecules influences the  $^{13}\text{C}$  chemical shift of the interior methylene groups of the alkyl chains. A previous study<sup>24</sup> has shown that the carbon atoms of *n*-alkanes gave a resonance at  $\sim 30$  ppm in solution, where trans and gauche conformations coexist, but in the crystalline solid, a downfield shift of about 3–4 ppm is observed for an all-trans conformation. Thus, we assign the resonance at 33.2 ppm in Figure 3 to those internal methylenes with all-trans conformations and the resonance at 31.0 ppm to those methylenes having mixed gauche and trans conformations. The ordered all-trans conformation observed for the 1:1 TMAOH/CTAB surfactant–silicate mesophase but absent for the previous as-synthesized MCM-41 material<sup>13</sup> indicates that higher temperature also increases the local molecular ordering of the bound surfactant.

The NMR resonances associated with the internal methylenes of the alkyl chain in Figure 3 can be deconvoluted into two peaks at 33.2 and 31.0 ppm to quantify the attendant chain conformations. The area ratio of the ordered conformation at 33 ppm (all-trans) to the disordered conformation at 31.0 ppm (mixed gauche and trans) is  $\sim 1.0$  for the 1:1 TMAOH/CTAB surfactant–silicate mesophase with an uncertainty of  $\pm 10\%$ . Furthermore, the fractional number of chains in the gauche conformation can be calculated approximately from the chemical shifts and the area ratios of resonances at 33.2 and 31.0 ppm on the basis of the so-called  $\gamma$ -gauche effect.<sup>21</sup> In the solid state, the  $^{13}\text{C}$  chemical shift is determined by the conformation and the packing density of the alkyl chains in addition to the chemical structure. The chemical shift of the alkyl chain methylene groups depends on the conformation of the two  $\gamma$

positions: trans–trans, trans–gauche/gauche–trans, or gauche–gauche. This so-called  $\gamma$ -gauche effect<sup>24</sup> generally leads to a low-field chemical shift of approximately 4.5 ppm for a methylene unit in a trans–trans conformation compared to that in a trans–gauche conformation and approximately 9 ppm compared to that in a gauche–gauche conformation. Chemical shifts have been used to calculate the fractional content of gauche conformations for stiff macromolecules with flexible side chains.<sup>21</sup> Using a similar method, the fractional number of chains in a gauche conformation was calculated to be approximately 16% for surfactant molecules in the 1:1 TMAOH/CTAB mesophase.

Although changes in the chemical shift associated with resonances at 31.0 and 33.2 ppm provide conformational information about the alkyl chains, the chemical shifts alone cannot quantitatively describe the rigidity of the alkyl chain. The conformation and dynamics of surfactant chains can be further studied using relaxation-time measurements. Figure 4 gives contact-time array spectra; the corresponding values of integrated peak areas for the 31.0 and 33.2 ppm resonances are plotted as a function of the  $^1\text{H}$ – $^{13}\text{C}$  cross-polarization contact time. The integrated signal intensity for both resonances shows an initial increase for a short contact time according to the relevant  $^1\text{H}$ – $^{13}\text{C}$  cross-polarization time constant,  $T_{\text{CH}}$ , which can be derived from the contact-time array measurements.<sup>25</sup> The relaxation time  $T_{\text{CH}}$  is directly related to the strength of  $^1\text{H}$ – $^{13}\text{C}$  dipole–dipole coupling, which depends on spatial proximity and molecular rigidity. Thus, the  $T_{\text{CH}}$  values associated with the alkyl chain resonances can be used to measure the rigidity of the alkyl chains in different conformations. A more rigid chain conformation gives a shorter  $T_{\text{CH}}$ . The much shorter  $T_{\text{CH}}$  value of 0.05 ms (Table 1) seen for the 33.2 ppm resonance contrasts with the  $T_{\text{CH}}$  of 0.13 ms observed for the 31.0 ppm resonance. This indicates that the alkyl chain in an ordered all-trans conformation at 33.2 ppm is much more rigid than the chain in the more disordered conformation at 31.0 ppm.

Table 1 also illustrates a comparison of the relaxation behavior for C16 alkyl chains in the locally ordered mesophase, in the mesophase without local ordering in the framework, and in the amorphous silicate. An all-trans conformation at  $\sim 33$  ppm is observed only for the C16 alkyl chain in the locally ordered mesophase (1:1 TMAOH/CTAB).  $T_{\text{CH}}$  values for the mixed gauche and trans conformation at 30 ppm are similar to that of the C16 alkyl chain in the mesophase composites with and without local ordering but are much smaller than that in the amorphous silicate. These results suggest that surfactant molecules have a higher degree of local ordering and less mobility

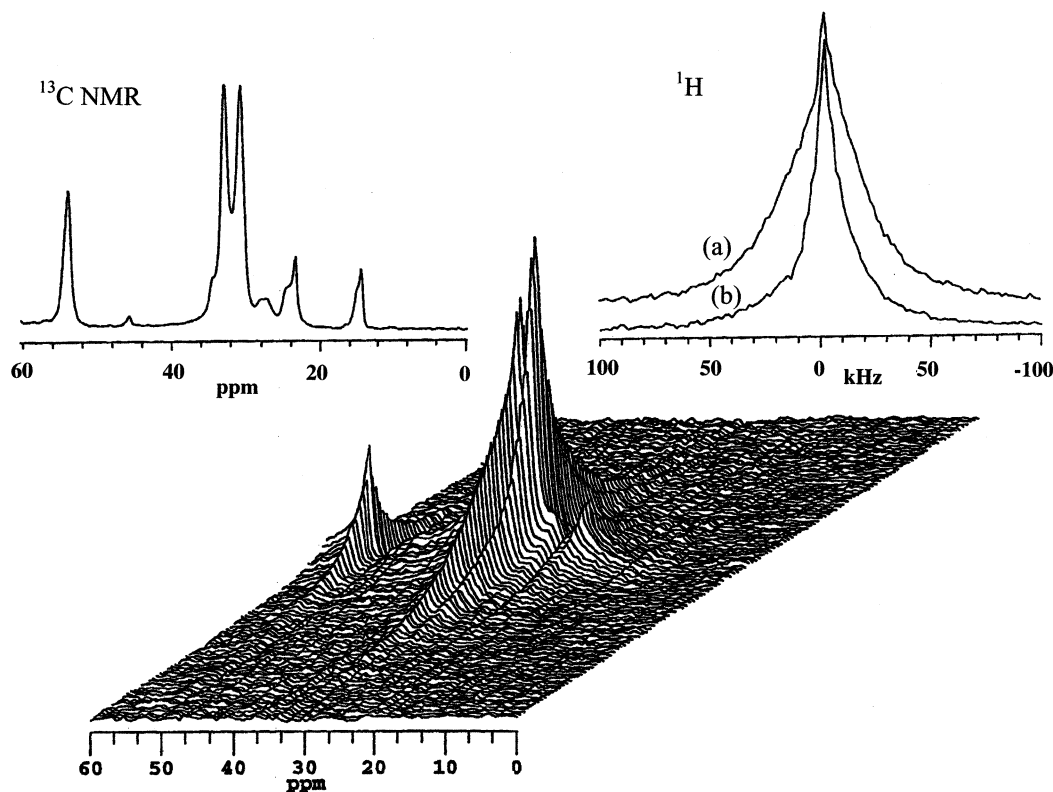


**Figure 5.** 2D WISE NMR spectra for the 1:1 TMAOH/CTAB mesophase. The upper-right inset displays the slices in the  $^1\text{H}$  dimension at 33.2 ppm (a) and 31.0 ppm (b) of the  $^{13}\text{C}$  resonances, and the single-pulse (SP) Bloch decay solid-state  $^{13}\text{C}$  NMR spectrum with proton decoupling is plotted in the upper-left inset.

**TABLE 1:  $T_{\text{CH}}$  Values (ms) Derived from Contact-Time Array Measurements**

	$T_{\text{CH}}$ (ms)	
	30 ppm	33 ppm
CTAB in the locally ordered mesophase	0.13	0.05
CTAC in the mesophase without local ordering	0.11 <sup>a</sup>	
CTAC in the amorphous silicate	0.38 <sup>b</sup>	

<sup>a</sup> For CTAC in the mesophase with no local ordering.<sup>20</sup> <sup>b</sup> For CTAC precipitated in the amorphous silica.<sup>20</sup>

when they are involved in the formation of both mesoscopically and locally ordered composites.

Since proton line widths determined from 2D WISE NMR measurements are directly related to the mobility of the surfactant chain without further data manipulation, 2D WISE NMR spectroscopy is used here to quantify chain mobility to confirm the results obtained from the cross-polarization time constant  $T_{\text{CH}}$  measurements.<sup>26</sup> In crystalline solids, the proton line widths are largely increased because of the strong dipolar interactions among the abundant proton spins. These line widths for crystalline solids typically range from 50 to 70 kHz. In semicrystalline or liquid environments, the proton line widths have decreased significantly because of the molecular motion that weakens the dipolar interaction. 2D WISE NMR spectra for the 1:1 TMAOH/CTAB mesophase composite are given in Figure 5. The upper-right inset displays the slices in the  $^1\text{H}$  dimension at 33.2 and 31.0 ppm of the  $^{13}\text{C}$  resonances corresponding to the all-trans and the mixed gauche and trans conformations, respectively, and the single-pulse (SP) Bloch decay solid-state  $^{13}\text{C}$  NMR spectrum with proton decoupling for the 1:1 TMAOH/CTAB mesophase composite is plotted in

the upper-left inset. The observation of a broader  $^1\text{H}$  NMR line width of 30 kHz (fwhm) for the 33.2 ppm resonance in comparison to that of 13 kHz (fwhm) for the 31.0 ppm resonance in the  $^{13}\text{C}$  NMR spectrum suggests that the alkyl chain in an all-trans conformation for the 1:1 TMAOH/CTAB mesophase composite has a higher degree of rigidity than the alkyl chain in a mixed gauche and trans conformation, in agreement with the results obtained from the  $T_{\text{CH}}$  measurements. However, the line width for the all-trans chain in the 1:1 TMAOH/CTAB mesophase is smaller than that for a typical crystalline solid, indicating that the oriented chains are undergoing motion about the chain axes. This suggests that crystalline-like conformational ordering does not necessarily correspond to crystalline-like rigidity.

Small tetraalkylammonium hydroxides such as TMAOH are commonly used as one of the essential ingredients in MCM-41 syntheses, where long-chain CTAB surfactant molecules serve as templating agents for the formation of mesophase composites. Both  $\text{TMA}^+$  and  $\text{OH}^-$  ions dissociated from TMAOH molecules in sol-gel solutions are believed to assist the formation of surfactant-silicate mesophase composites,<sup>13</sup> whereas these small tetraalkylammonium ions are used to template the synthesis of crystalline zeolite materials. Since small tetraalkylammonium hydroxides play different roles in the syntheses of mesophase composites and crystalline zeolites, it is important to examine the function of such ions in the synthesis of locally ordered surfactant-silicate mesophase composites.

Figures 6, 7, and 8 show XRD,  $^{29}\text{Si}$ , and  $^{13}\text{C}$  NMR spectra for the surfactant-silicate mesophase composites with molar ratios of 1:1 TPAOH/CTAB, 1:1 TBAOH/CTAB, and 4:1 TBAOH/CTAB, respectively. In comparison with the data (Figures 1–3) for the 1:1 TMAOH/CTAB mesophase, the corresponding XRD,  $^{29}\text{Si}$ , and  $^{13}\text{C}$  NMR spectra (Figures 6–8) for both 1:1 TPAOH/CTAB and 1:1 TBAOH/CTAB mesophase

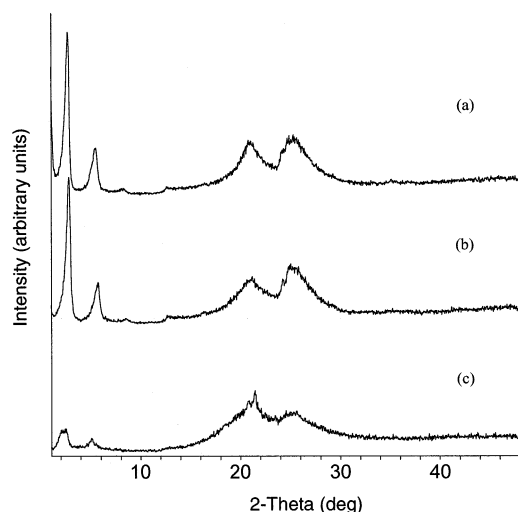


**Figure 6.** XRD spectra for surfactant-silicate mesophase composites with molar ratios of 1:1 TPAOH/CTAB (a), 1:1 TBAOH/CTAB (b), and 4:1 TBA/CTAB (c) prepared under hydrothermal conditions at 150 °C.

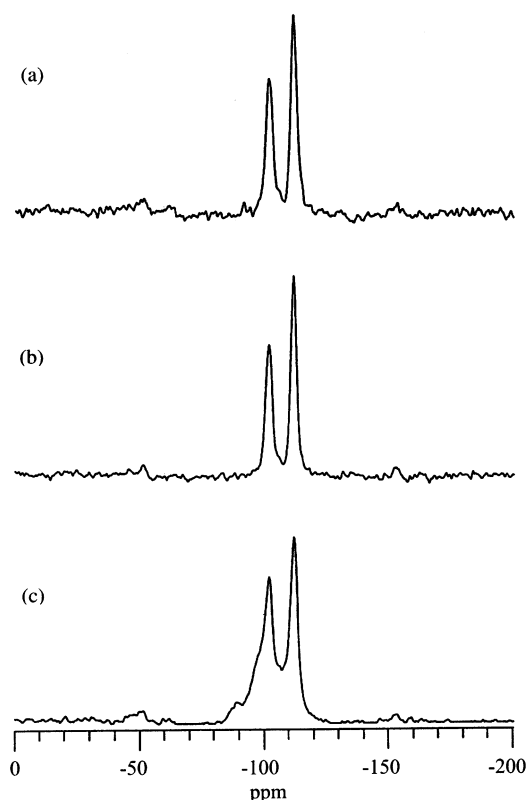


**Figure 7.**  $^{29}\text{Si}$  NMR spectra for surfactant-silicate mesophase composites with molar ratios of 1:1 TPAOH/CTAB (a), 1:1 TBAOH/CTAB (b), and 4:1 TBA/CTAB (c) prepared under hydrothermal conditions at 150 °C.

composites are nearly identical, indicating that the local molecular ordering does not depend on the size of the tetraalkylammonium ions. However, the line width for the  $\text{Q}^3$  resonance in the  $^{29}\text{Si}$  NMR spectrum (Figure 7c) for the 4:1 TBAOH/CTAB mesophase is broader than that for the 1:1 TBAOH/CTAB mesophase (Figure 7b), indicating reduced local ordering in the silica framework for the 4:1 TBAOH/CTAB mesophase. In addition, the  $^{13}\text{C}$  spectrum (Figure 8c) shows slightly broader resonances at 33.2 and 31.0 ppm and a correspondingly decreased amount of the ordered all-trans conformation for the 4:1 TBAOH/CTAB in comparison to that for the 1:1 TBAOH/

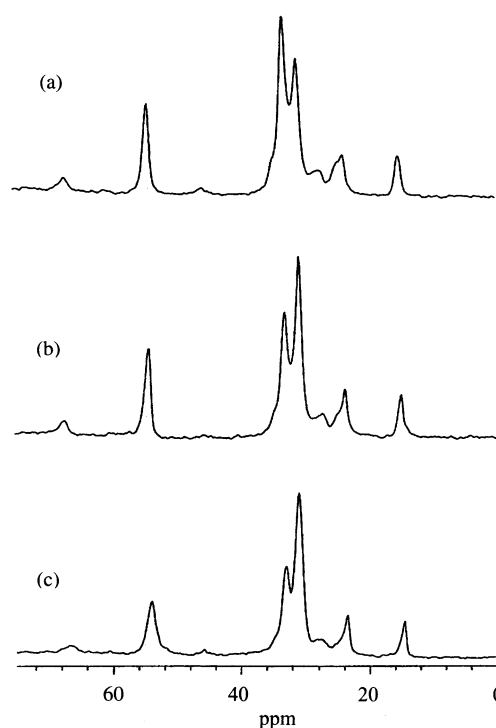


**Figure 8.** Solid-state  $^{13}\text{C}$  MAS NMR spectra for surfactant-silicate mesophase composites with molar ratios of 1:1 TPAOH/CTAB (a), 1:1 TBAOH/CTAB (b), and 4:1 TBA/CTAB (c) prepared under hydrothermal conditions at 150 °C.

CTAB mesophases. Furthermore, low-angle XRD peaks in Figure 6c for the 4:1 TBAOH/CTAB mesophase are also weaker and broader than for the 1:1 TBAOH/CTAB mesophase, in agreement with both the  $^{13}\text{C}$  and  $^{29}\text{Si}$  NMR spectra. These results suggest that local molecular ordering starts to decrease as the molar ratio of tetraalkylammonium ions to CTAB is increased above a mole ratio of 1. However, when the molar ratio of tetraalkylammonium ions to surfactant CTAB is decreased to 0.2, such local molecular ordering disappears. In addition, no ordered layered structures were observed when the molar ratio of TMAOH to CTAB was decreased to 0.2, indicating that a certain concentration of TMAOH is required to assist the formation of mesoscopically ordered silicates. The  $^{29}\text{Si}$  NMR spectrum given in Figure 9a for the 0.2:1 TMAOH/CTAB mesophase shows broad features, resembling  $^{29}\text{Si}$  NMR spectra for amorphous silica. Therefore, the relative amount of tetraalkylammonium ions to surfactant molecules is a critical factor that influences local molecular ordering in surfactant-silicate mesophase composites. Furthermore, the surfactant chain length was also found to influence the local molecular ordering. Figure 9b shows the  $^{29}\text{Si}$  NMR spectrum for the surfactant-silicate mesophase prepared using  $\text{C}_{10}\text{H}_{21}(\text{CH}_3)_3\text{NBr}$  as the surfactant instead of  $\text{C}_{16}\text{H}_{33}(\text{CH}_3)_3\text{NBr}$  (CTAB) at a 1:1 molar ratio of TMAOH to surfactant under the same conditions. Broad amorphous-like silica features shown in Figure 9b suggest that the surfactant chain length significantly influences the local ordering in the silica framework.

The previous study reported local molecular ordering in the silica framework for the layered surfactant-silicate mesophase.<sup>17</sup> In comparison to this previous work,<sup>17</sup> the current study shows similar XRD and  $^{29}\text{Si}$  NMR spectra, further confirming the existence of local ordering in the silica framework. Two broad high-angle reflections observed previously in the XRD spectra at 0.41 and 0.35 nm were attributed to the attendant organization of strongly interacting surfactant molecules with the silica

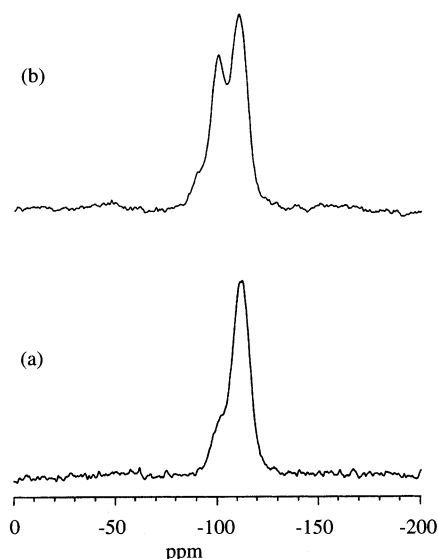


**Figure 9.**  $^{29}\text{Si}$  NMR spectra for the 0.2:1 TMAOH/CTAB surfactant-silicate mesophase (a) and the mesophase prepared using a 1:1 molar ratio of TMAOH/C10 surfactant (b).

framework.<sup>13,17</sup> Similar high-angle XRD reflections at 0.42 and 0.35 nm (Figure 1) were also observed in this study. The characteristic features of the local ordering from both  $^{29}\text{Si}$  and  $^{13}\text{C}$  NMR spectra seem to correlate with these high-angle XRD reflections. In another words, the narrow features observed in  $^{29}\text{Si}$  NMR spectra, characteristic of the locally ordered silica framework, are always accompanied by well-resolved all-trans chain conformations in  $^{13}\text{C}$  NMR spectra and high-angle reflection peaks in XRD for the surfactant-silicate mesophase composites prepared in this study. However, these characteristic features are absent in both XRD spectra and  $^{13}\text{C}$  as well as  $^{29}\text{Si}$  NMR spectra for the mesoporous silicates composed of a disordered framework. Thus, any one of several features can be used to identify the existence of local ordering in mesoporous silicates.

Contrasting processing conditions (chemical precursors, compositions, and temperatures) were used to prepare surfactant-silicate mesophase composites with a locally ordered framework in a previous investigation<sup>17</sup> and in this work. The main reagents for the 1:1 TMAOH/CTAB mesophase are CTAB,  $\text{SiO}_2$  (Hi-Sil 233 as a silica source), TMAOH, and  $\text{H}_2\text{O}$  with a molar ratio of 1.0 CTAB/3.0  $\text{SiO}_2$ /1.0 TMAOH. The previous study used CTAB, TMOS (as a silica source), HBr,  $\text{CH}_3\text{OH}$ , and  $\text{H}_2\text{O}$  with a molar ratio of 1.0 CTAB, 1.4  $\text{SiO}_2$ /1.0 TMAOH. No other solvents besides  $\text{H}_2\text{O}$  and a higher  $\text{SiO}_2$ /CTAB ratio were used in this synthesis. Additionally, temperatures used in both studies are different. As a result of the higher processing temperature of 150 °C used in this work (135 °C in the previous study), the rate of formation of the locally ordered mesostructures at 150 °C is faster. Only 24 h at 150 °C was required to achieve similar molecular ordering to that observed in the previous study (48 h at 135 °C).

In contrast to the previous XRD data that indicated a mixture of segregated MCM-41 and zeolite crystalline phases,<sup>14-16</sup> no sharp XRD features, characteristic of zeolite-like materials, were observed in our synthesis of surfactant-silicate mesophases with local ordering, indicating that no zeolite materials are made during the syntheses of the locally ordered surfactant-silicate mesophase composites. Thus, the small tetraalkylammonium hydroxides used in this study did not template for the zeolite structure. In addition, strongly interacting surfactant molecules with the silica framework (revealed in XRD spectra for the

locally ordered mesophase composites) make it impossible to form a macroscopic segregated phase of surfactant and silica species. Unique all-trans conformations observed in  $^{13}\text{C}$  NMR spectra for the surfactant molecules most likely result from a strong interaction between silica and surfactant species and from the restricted motion when surfactant molecules are confined within the layered structure. Such surface confinement has been observed previously.<sup>26</sup> Therefore, it is reasonable to assume that surfactant molecules are oriented themselves within ordered 2D silica sheets of these surfactant-silicate mesophase composites.

#### 4. Conclusions

In this work, we have successfully synthesized layered surfactant-silicate mesophase composites with local molecular ordering using surfactant-templated synthetic routes under hydrothermal processing conditions. Local molecular ordering was observed by solid-state NMR and X-ray diffraction techniques both in the bound surfactant and in the inorganic framework associated with these layered surfactant-silicate mesophase composites. The dynamics and chain mobility of surfactant molecules at interfaces have also been determined using NMR chemical-shift analyses, relaxation times, and 2D WISE measurements. Several critical factors including the temperature, the length of the surfactant chains, and the relative amount of TMAOH to surfactant are found to influence local molecular ordering. All surfactant-silicate mesophase composites exhibiting local molecular ordering share characteristic features in their respective XRD,  $^{13}\text{C}$ , and  $^{29}\text{Si}$  NMR spectra.

**Acknowledgment.** We thank Dr. J. Liu and Dr. Y. Shin for helpful discussions and Gloria Ruiz for helping with figure preparation. This work has been supported by the Division of Materials Sciences and Engineering, Office of Basic Energy Sciences, U.S. Department of Energy (USDOE). The research described in this paper was performed in part in the Environmental Molecular Sciences Laboratory, a national scientific user facility sponsored by the U.S. Department of Energy's Office of Biological and Environmental Research located at Pacific Northwest National Laboratory in Richland, WA. Pacific Northwest National Laboratory is a multiprogram national laboratory operated for the U.S. DOE by Battelle Memorial Institute under contract DE-AC06-76RLO 1830.

#### References and Notes

- (1) Beck, J. S.; Vartuli, J. C.; Roth, W. J.; Leonowicz, M. E.; Kresge, C. T.; Schmitt, K. D.; Chu, C. T.-W.; Olson, D. H.; Sheppard, E. W.; McCullen, S. B.; Hihhins, J. B.; Schlenker, J. L. *J. Am. Chem. Soc.* **1992**, *114*, 10834.
- (2) Kresge, C. T.; Leonowicz, M. E.; Roth, W. J.; Vartuli, J. C.; Beck, J. S. *Nature (London)* **1992**, *359*, 710.
- (3) Vartuli, J. C.; Kennedy, G. J.; Kresge, C. T.; Roth, W. J.; Schramm, S. E. *Chem. Mater.* **1994**, *6*, 1816. Vartuli, J. C.; Schmitt, K. D.; Kresge, C. T.; Roth, W. J.; Leonowicz, M. E.; McCullen, S. B.; Hellring, D. C.; Beck, J. S.; Schlenker, J. L.; Olson, D. H.; Sheppard, E. W. *Chem. Mater.* **1994**, *6*, 2317.
- (4) Beck, J. S.; Vartuli, J. C.; Kennedy, G. J.; Kresge, C. T.; Roth, W. J.; Schramm, S. E. *Chem. Mater.* **1994**, *6*, 1816.
- (5) Huo, Q.; Margolese, D. I.; Ciesla, U.; Feng, P.; Gier, T. E.; Sieger, P.; Leon, R.; Petroff, P. M.; Schuth, F.; Stucky, G. D. *Nature (London)* **1994**, *368*, 317. Huo, Q.; Margolese, D. I.; Ciesla, U.; Demuth, D. G.; Feng, P.; Gier, T. E.; Sieger, P.; Chmelka, B. F.; Stucky, G. D. *Chem. Mater.* **1994**, *6*, 1176.
- (6) Tanev, P. T.; Pinnavaia, T. J. *Science (Washington, D.C.)* **1995**, *267*, 865.
- (7) Firouzi, A.; Kumar, D.; Bull, L. M.; Besier, T.; Sieger, P.; Huo, Q.; Walker, S. A.; Zasadzinski, J. A.; Glinka, C.; Nicol, J.; Margolese, D.; Stucky, G. D.; Chmelka, B. F. *Science (Washington, D.C.)* **1995**, *267*, 1138.
- (8) Monnier, A.; Schuth, F.; Huo, Q.; Kumar, D.; Margolese, D.; Mawell, R. S.; Stucky, G. D.; Krishnamurty, M.; Petroff, P.; Firouzi, A.; Janicke, M.; Chmelka, B. F. *Science (Washington, D.C.)* **1993**, *261*, 1299.



- (9) Liu, J.; Kim, A. Y.; Virden, J. W.; Bunker, B. C. *Langmuir* **1995**, *11*, 689.
- (10) Stucky, G. D.; Monnier, A.; Schuth, F.; Huo, Q.; Margolese, D.; Kumar, D.; Krishnamurty, M.; Petroff, P.; Firouzi, A.; Janicke, M.; Chmelka, B. F. *Mol. Liq. Cryst.* **1994**, *240*, 187.
- (11) Chen, C.; Li, H.; Davis, M. E. *Microporous Mater.* **1993**, *2*, 17.
- (12) Cheng, C. F.; Luan, Z.; Kinowski, J. *Langmuir* **1995**, *11*, 2815.
- (13) Huo, Q.; Margolese, D.; Stucky, G. D. *Chem. Mater.* **1996**, *8*, 1147.
- (14) Huang, L.; Guo, W.; Deng, P.; Xue, Z.; Li, Q. *J. Phys. Chem. B* **2000**, *104*, 2817.
- (15) Karlsson, A.; Stöcker, M.; Schmidt, R. *Microporous Mesoporous Mater.* **1999**, *27*, 181.
- (16) Kloetstra, K. R.; van Bekkum, H.; Jansen, J. C. *Chem. Commun.* **1997**, *23*, 2281.
- (17) Christiansen, S. C.; Zhao, D.; Janicke, M. T.; Landry, C. C.; Stucky, G. D.; Chmelka, B. F. *J. Am. Chem. Soc.* **2001**, *123*, 4519.
- (18) Kolodziejski, W.; Corma, A.; Navarro, M. T.; Pariente, J. *Solid-State NMR* **1993**, *2*, 253.
- (19) Steel, A.; Carr, S. W.; Anderson, M. W. *Chem. Mater.* **1995**, *7*, 1829.
- (20) Wang, L.-Q.; Liu, J.; Exarhos, G. J.; Bunker, B. C. *Langmuir*, **1996**, *12*, 2663.
- (21) Clauss, J.; Schmidt-Rohr, K.; Adam, A.; Boeffel, C.; Spiess, H. W.; *Macromolecules* **1992**, *25*, 5208.
- (22) Dixon, W. T. *J. Chem. Phys.* **1982**, *77*, 1800.
- (23) Engelhardt, G.; Michel, D. *High-Resolution Solid-State NMR of Silicates and Zeolites*; Wiley & Sons: New York, 1987.
- (24) (a) Earl, W. L.; VanderHart, D. L. *Macromolecules* **1979**, *12*, 762.
- (b) Tonelli, A. E.; Schilling, F. C. *Acc. Chem. Res.* **1981**, *14*, 3.
- (25) Demco, D. E.; Tegenfeldt, J.; Waugh, J. S. *Phys. Rev. B* **1974**, *11*, 4133.
- (26) Wang, L.-Q.; Liu, J.; Exarhos, G. J.; Flanigan, K. Y.; Bordia, R. *J. Phys. Chem. B* **2000**, *104*, 2810.